Electronic Supplementary Information

Hazardous o-toluidine mineralization by photocatalytic bismuth doped ZnO slurries

G. Cappelletti,[a*] V. Pifferi,[a] S. Mostoni,[a] L. Falciola,[a] C. Di Bari,[a‡] F. Spadavecchia,[a†] D. Meroni,[a] E. Davoli[b] and S. Ardizzone[a]

1. Impregnation method

All Bi-doped samples were prepared using a commercial zinc oxide powder (available from Sigma Aldrich) by exploiting an impregnation method. This method is based on wetting the zinc oxide nanopowders by adding different volume of 0.1 M $Bi(NO_3)_3 \cdot 5H_2O$ in HNO_3 65% in order to obtain three different Bi/Zn molar ratios (0.01, 0.02 and 0.03). Then, the powders were dried in an oven at 90°C and calcined at 400°C for 6 hours. The doping of the bare sample is evident by the colour change from white to yellowish.

2. Morphological and structural characterizations

The powders (both bare and doped) were characterized by morphological (SEM) and structural (XRD) points of view. These characterizations allow to finely compare the bare and doped nanopowders, in order to understand which modifications are provoked by the addition of the bismuth as dopant species.

X-ray powder diffraction lines were collected with a Philips PW 3710 diffractometer (PW 1830 generator, PW 3020 vertical goniometer) equipped with graphite reflected beam monochromator and using Cu Kα radiation (λ_1=1.54178 Å, λ_2=1.54443 Å). The X-ray diffractometer was operated in reflection mode at 40 kV and 40 mA. For all the studied samples, powder patterns were collected between 20° and 90° with a counting time of 20 seconds and a 0.08° step. Figure S1 shows that the wurzite phase is the predominant one in the zinc oxide bare sample; a second segregate phase, the bismite (Bi_2O_3), appears when the doped samples are considered. The peak referred to the bismite is particularly appreciable when the molar ratio Bi/Zn is higher (molar ratios > 0.01).

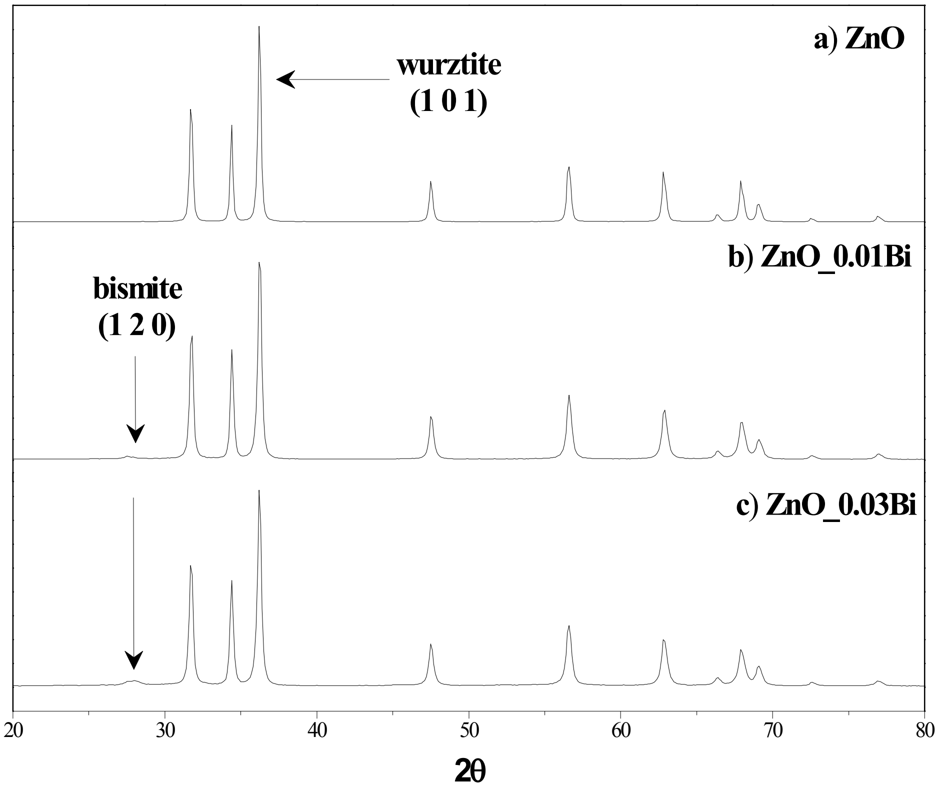

FIGURE S1

Further, energy-filtering transmission electron microscope (EFTEM) was used to study both the morphology of the samples. Bismuth loadings was assessed by a Energy-dispersive X-ray spectroscopy (EDS – Oxford INCA Energy TEM 200) line profile and maps coupled with high angular annular dark field scanning electron microscopy (HAADF-(S)TEM). All the specimens were suspended in isopropanol and sonicated 25 minutes. A drop of the fine suspensions were then deposited onto a holey carbon coated copper grid and dried overnight. All doped samples show compact agglomerates and it seems that bismuth allows the formation of wires not homogeneously distributed (Figure S2). Furthermore, using EDX the effective presence of the bismuth and its distribution all over the powders was evaluated.

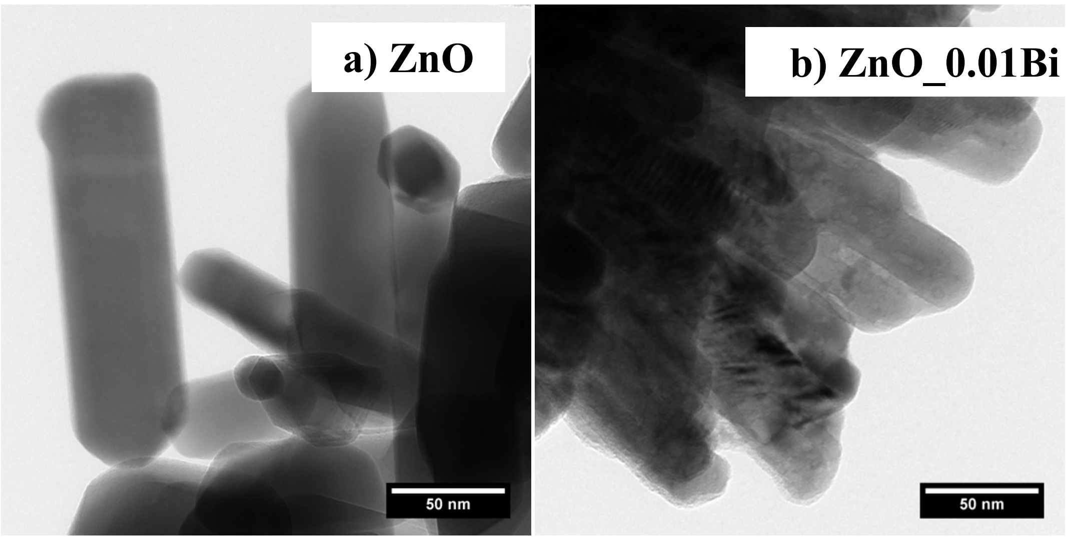

FIGURE S2

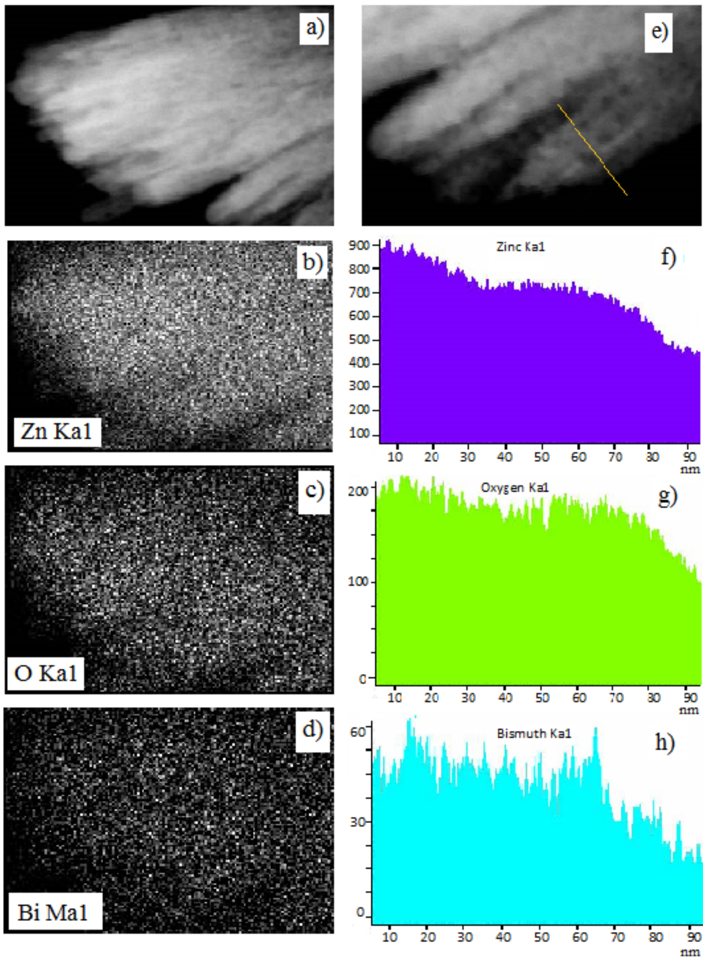

FIGURE S3

3. Degradation experiments

All *o*-toluidine degradation tests were carried out in slurries with a concentration of 0.3 g L^{-1} at 25°C and at spontaneous pH (around 8.0). Under the present experimental conditions, no release or leaching both of Zn and/or Bi species was determined. A 600 mL cylindrical jacketed glass reactor was utilized. The experiments were carried out for 6 hours under either UV (Jesosil HG 500 W, λ = 280-400 nm, effective power density 57.5 mW cm^{-2}) or solar (Lot oriel, effective power density: 1mW cm^{-2}, λ = 280-400 nm; 14 $mWcm^{-2}$ λ = 400-800 nm) irradiation sources after 20 minutes of dark adsorption. *o*-Toluidine was the target compound, available by Sigma-Aldrich, with an initial concentration of 25 ppm. Direct photolysis under UV irradiation was negligible. No direct reusability tests on exhaust catalyst have been performed; however, exhaust catalyst containing Bi, after washing with alcohols or submitted to a further calcinations step, presents an activity fully comparable with a fresh catalyst.

The progressive degradation of *o*-toluidine over time (sampling aliquots every 90 minutes) was monitored by measuring the disappearance and mineralization percentage, by using LSV (linear sweep voltammetry) and TOC (total organic carbon) analyses, respectively. In voltammetric analysis a 3 electrodes cell was used, in which the working electrode was a glassy carbon covered with Carbon NanoTubes (CNTs); a filament of Pt and an Ag/AgCl electrode as counter and reference electrodes, respectively. HCl 0.1 M was used as the supporting electrolyte and the potential was varied from +0.60 V to +1.00 V (SCE). The *o*-toluidine molecule was detected at about 0.9-0.95 V (Figure S4); excellent results were obtained, characterized by linear increasing of *o*-toluidine peaks and a calibration plot with very good correlation, as shown in Fig. S4.

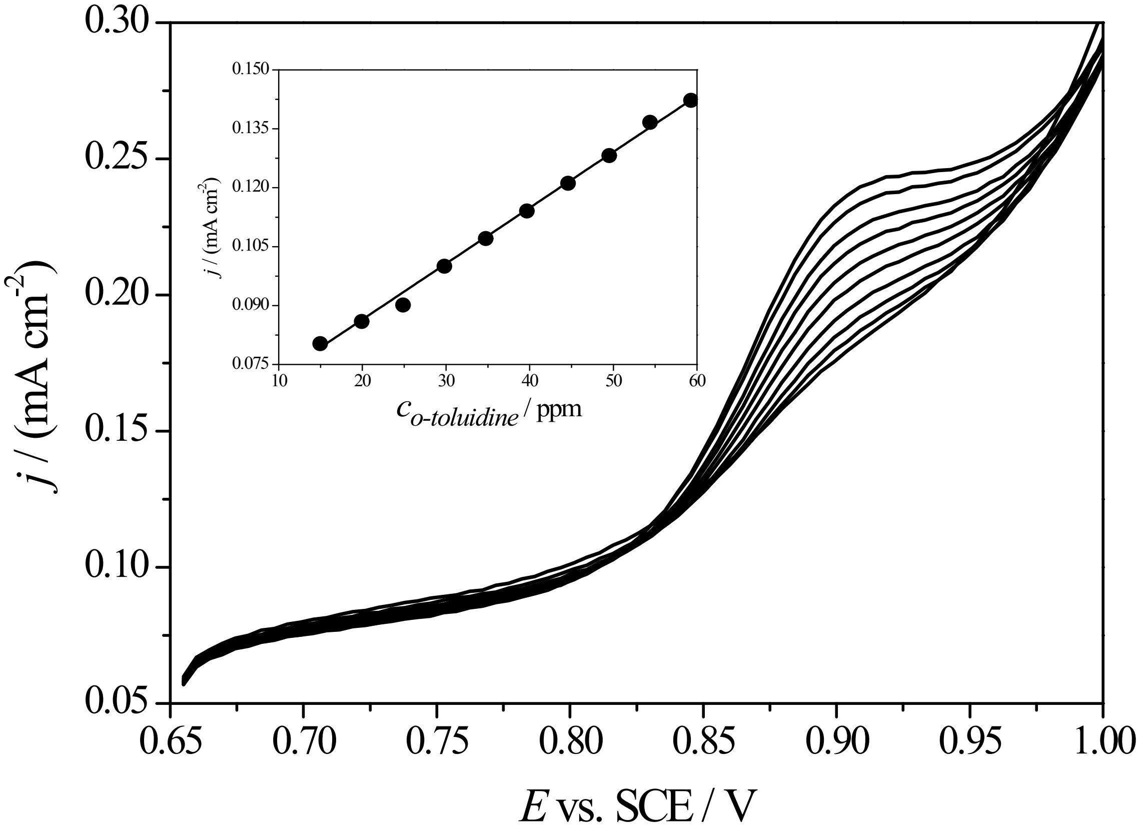

FIGURE S4

4. Oxidation intermediate products

HPLC-MS/MS experiments were performed on an API-3000 (AB Sciex) and on a 6410 Agilent instrument. High resolution MS experiments on a nano-ESI/FTMS (LTQ XL Orbitrap, Thermo Fisher). HPLC separations were obtained with a RP column (Eclipse XDB-C18) with water methanol phase (70:30). *o*-Toluidine dimer identification was done by high resolution MS experiments. HPLC separation of the dimer is shown in Fig. S6a, the molecular ion, and S6b, methyl loss from the molecular ion. Chromatographic peak identification was performed by high resolution mass assignment where it is shown molecular ion elemental composition measurements within 1 ppm accuracy error (c). The methyl loss appearing at m/z 195.0911 was identified with the same accuracy (data not shown).

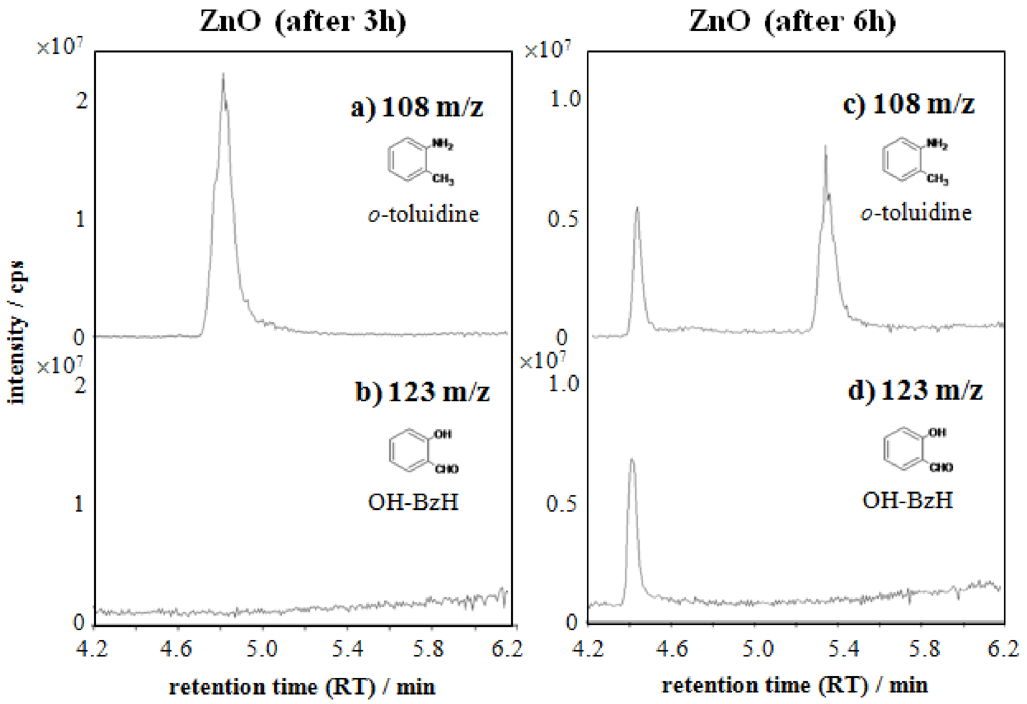

FIGURE S5

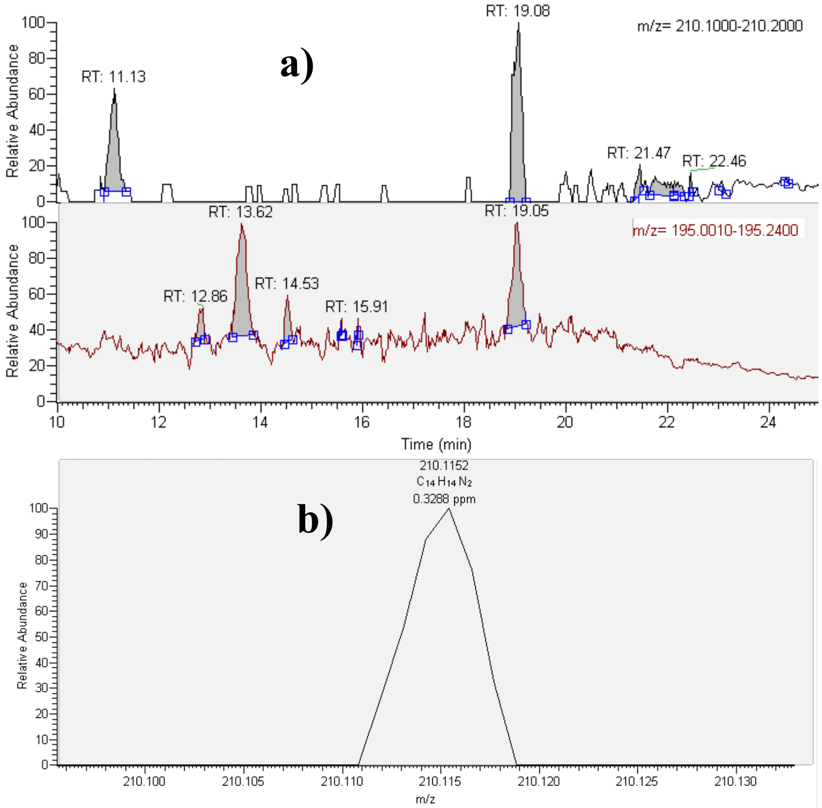

FIGURE S6

5. Photocurrent measurements

Photocurrent measurements were performed by using ZnO thin films prepared by spin-coating a 2-ethanol suspension of the oxide powder with a Spin150 spin-coater (SPS, ATP GmbH, 2000 rpm for 20 s, 8 layers) onto flourine-doped tin oxide (FTO) conducting glass (Aldrich, 2.3 mm thick, ~7 Ω/sq surface resistivity). The as-prepared films were finally sintered at 400 °C in air for 1 h. The photocurrent developed by irradiating the photoanode (ZnO) with UV light [see photocatalytic setup section] was recorded by a microIII Autolab potentiostat/galvanostat (EcoChemie, The Netherlands). The dark/light alternation was repeated for at least 6 times, in order to obtain reproducible transient patterns. The photoelectrochemical cell was a three compartment one, with two counter electrodes, both consisting in a Pt wire parallel to the working electrode, a saturated calomel electrode as reference, a Luggin capillary in order to minimize the ohmic drop and a ZnO film located in the middle of the cell as working electrode. All the measurements have been carried out in N_2 atmosphere, after degassing the cell with nitrogen flow for at least 10 minutes.

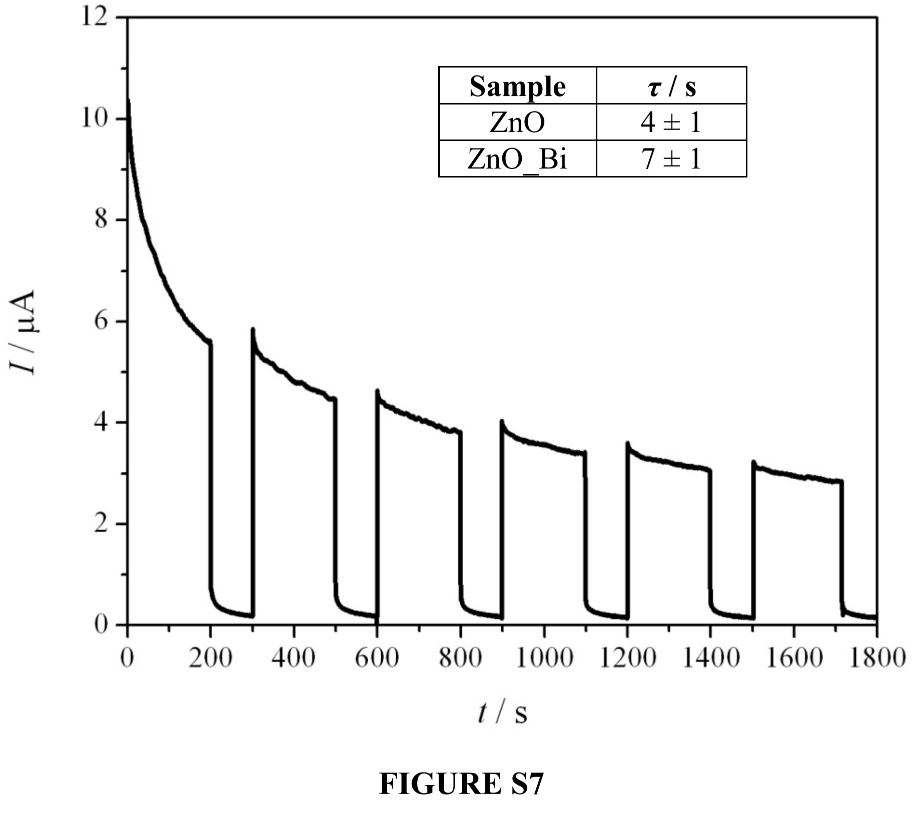

Sample	***τ* / s**
ZnO	4 ± 1
ZnO_Bi	7 ± 1

FIGURE S7

Preliminary linear sweep voltammetries (LSV) have been recorded in the same experimental conditions at a scan rate of 50 mV s^{-1} in order to evaluate the potential at which the photocurrent is constant to be chosen as working potential for the chronoamperometric tests (1.0 V SCE).

The typical chronoamperometric output of the experiment is shown in Fig. S7 in the case of ZnO material. The decay observed for all the tested materials indicates that electron-hole recombination processes are occurring. The photocurrent transient can be evaluated by considering the following first-order kinetic equation (inset of Fig. S7) for the first 15 s of decay:

$$I(t) = Ae^{-\frac{t}{\tau}} + I_f$$

where A is a constant, $I(t)$ is the current normalized by both the stationary and the dark values, I_f the current after 15 s and τ is the transient time constant, related to the mechanism of electron transport; τ gives indications about the time for charge recombination processes in the semiconductor film.

6. Optical properties

Optical properties were determined by diffuse reflectance spectroscopy using a Jasco UV/VIS/NIR spectrometer (model V-570), equipped with an integrating sphere of barium sulphate. The source for UV light is a deuterium lamp (190-350 nm); for VIS/NIR a tungsten iodide lamp was used (340-2500 nm). The instrument is capable of measuring alternatively the diffused light from the sample and from a reference; the barium sulphate is used to collect the diffused light for the measurement and to light the sample uniformly in a cell ISN-470.

Figure S8 shows the Kubelka-Munk elaboration of the diffuse reflectance spectra of both bare and Bi-doped samples. These results demonstrate that bismuth is able to shift the light adsorption from UV to solar light, lowering the "apparent" band gap values. Consequently bismuth doping is fundamental for improving photocatalytic properties of doped samples under visible light.

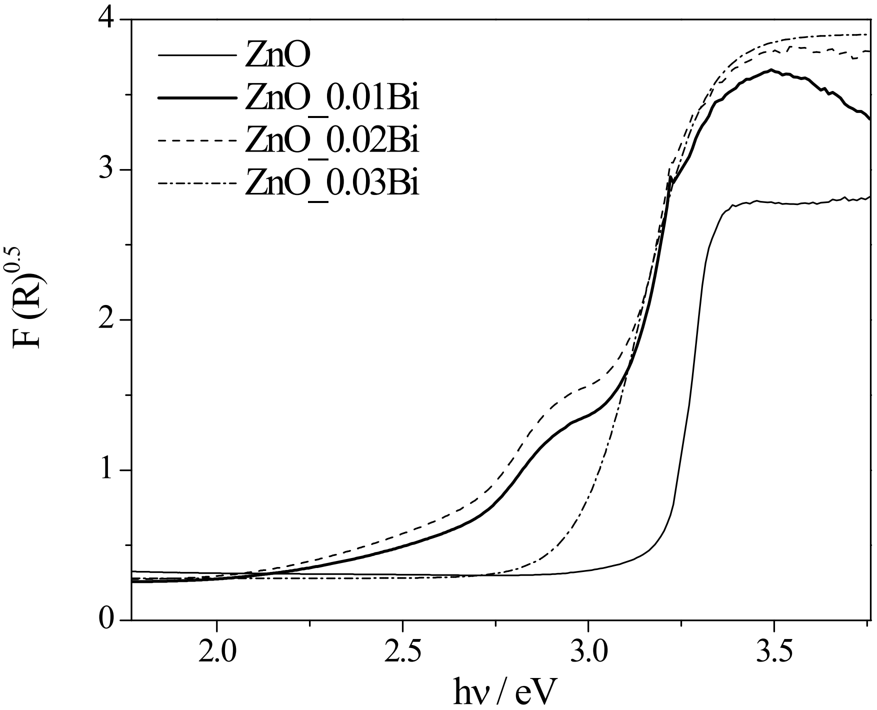

FIGURE S8